

RECOMMENDED METHODS FOR SETTING MISSION CONJUNCTION ANALYSIS HARD BODY RADII

Alinda K. Mashiku* and Matthew D. Hejduk†

For real-time conjunction analysis (CA) operations, computation of the Probability of Collision (P_c) typically depends on the state vector, its covariance, and the combined hard body radius (HBR) of both the primary and secondary space objects. However, most algorithmic approaches that compute the P_c use generic conservatively valued HBRs that may tend to go beyond the physical limitations of both spacecraft, enough to drastically change the results of a conjunction assessment mitigation decision. On the other hand, if the attitude of the spacecraft is known and available, then a refined HBR can be obtained that could result in an improved and accurate numerically-computed P_c value. The goal of this analysis is to demonstrate the various number of different HBR calculation techniques and the resulting calculated P_c values obtained, based on spacecraft orientations in the encounter or conjunction plane at the time of closest approach (TCA). Since in most conjunctions the secondary object tends to be a space debris object and thus orders of magnitude smaller than the primary, the greatest operational benefit is wrought by developing a better size estimate and representation for the primary object. We present an analysis that includes the attitude information of the primary object in the HBR calculation and evaluating the resulting P_c values for conjunction analysis and risk assessment decision-making.

INTRODUCTION AND BACKGROUND

The probability of collision (P_c) in a close approach event is a scalar numerical output that is computed using the state vector estimates of the spacecraft, the associated covariance, and the hard body radius (HBR). The covariance quantifies the uncertainty in the state vector; however, there is no similar uncertainty value incorporated for the HBR. One could argue that since the dimensions of the primary spacecraft are typically known, one can assign a scalar HBR value from circumscribing a 3D sphere, based on the three dimensions of the primary spacecraft. However, this scalar value may not always be valid or physically representative, depending on the method used to calculate P_c .

Additionally, the majority of close approach events tend to be in the Low-Earth Orbit (LEO) regime. In LEO, the physics of the dynamics tend to differ compared to those in the geosynchronous (GEO) regime. In LEO, the spacecraft are much closer to the Earth and thus tend to travel at higher velocities; thus, an assumption of high relative conjunction velocities for most close encounters in LEO is quite reasonable. A profiling of the approximately 1.5M conjunctions

* NASA CARA Deputy Manager, NASA Goddard Space Flight Center, Code 595, 8800 Greenbelt Road, Greenbelt, Maryland 20771, USA.

† CARA Chief Engineer, Astrorum Consulting LLC, Waco, Texas 76712, USA.

in the CARA database gives the following distribution for conjunction relative velocities shown in Figure 1:

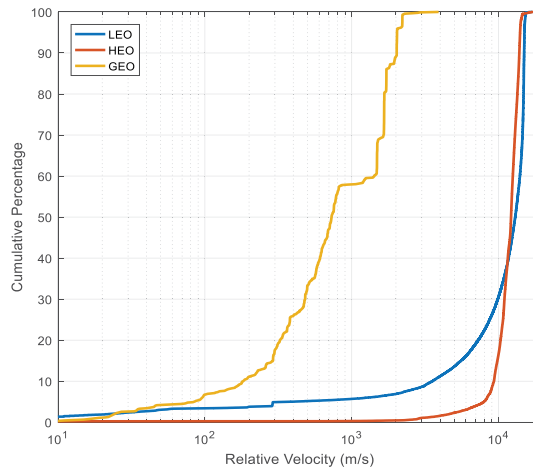


Figure 1. Relative velocity distributions for CARA conjunctions

With this assumption that a conjunction has high relative velocities between the objects in LEO, the conjunction geometry now allows the simplification of a three-dimensional encounter region to a 2-dimensional encounter plane, as explained in a number of references but capably summarized in Chan¹.

Given this simplification, the HBR is now a circumscribing circle on the encounter plane with the assumption of an instantaneous conjunction duration. With this two-dimensional approach, it becomes evident that for a given close approach with a secondary object, the encounter plane has three degrees of rotational freedom of the primary object, and thus the resultant area of the primary object projected on the encounter plane has the potential to vary widely, giving rise to HBR uncertainty ranges. However, if a given mission possesses quality attitude information for its spacecraft at the time of closest approach (TCA) of the conjunction, one would be able to incorporate the attitude information and determine the spacecraft's actual projected area into the conjunction plane, eliminating this source of uncertainty.

The goal of this analysis is to demonstrate the wide range of HBR that is possible to assign to a spacecraft, based on the particular HBR determination approach chosen. From these HBR ranges, and using the information from the attitude profile, a Pc range is thus available for various HBR definition profiles. The practice for many years, and an approach still followed for some primaries, is to use a static 20-meter HBR to represent the combined sizes of the primary and secondary objects. However, in most cases this approach can greatly overstate the combined size of the two objects and thus artificially inflate the Pc; Hence, there is therefore a benefit in working to develop more realistic HBR estimates.

In the probability of collision calculation, HBR (usually) represents the radius of a circular region circumscribing both the primary and secondary spacecraft in the conjunction plane. Given

that P_c is proportional to the HBR derived from the cross-sectional area, the goal is actually to arrive at a good estimate of the object's projected area rather than worrying about exact volume or shape. A similar analysis was also implemented in the investigation of the P_c given different projected areas of the International Space Station by Chan². In Figure 2, which is the standard conjunction plane diagram of a conjunction, the P_c calculation integral determines how much of the hard-body radius circle is contained within the probability density function of the combined covariance. Since the combined covariance is an infinitely-expanding probability density ellipse (or ellipsoid), there will always be a positive solution to this integral, although it is often very small or smaller than the computer's machine precision.

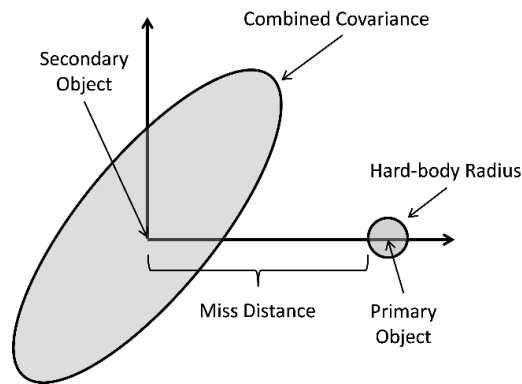


Figure 2. Hard-body Radius and Covariance schematic for Probability of Collision calculations

Similar approaches have been developed for determining averaged cross sectional area for modeling atmospheric drag. M. Matney of the NASA Orbital Debris Program Office demonstrated that all convex shapes will have an average projected area that is 25% of the surface area³. While it might be possible to perform such calculations analytically, the easiest approach may be to assemble a mock-up for a protected asset and run it through incremental rotations. It is likely sufficient to use the common shapes of flat plates, cylinders, and rectangular prisms (and maybe spheres as well) to construct the satellite models.

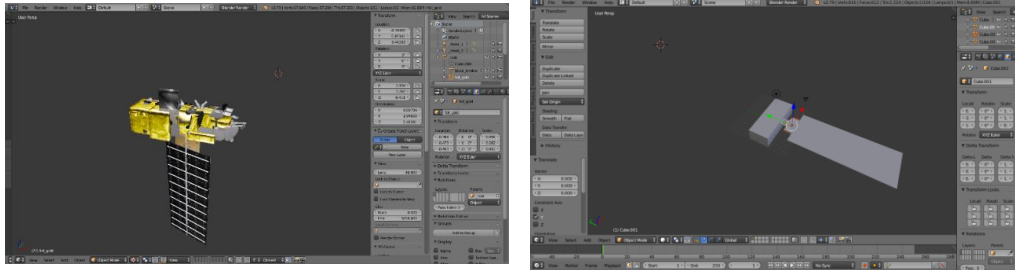
PRIMARY SATELLITE AREA PROJECTION METHODS

In this section, we present various approaches and assumptions considered in projecting a three-dimensional spacecraft unto a two-dimensional plane and how the HBR would then affect the P_c calculation at TCA. The first steps in this analysis effort involved the development and use of software that allows assembly of simple models of satellites, rotation through 2π steradians for each axis, and determining the confidence interval of the projected area on the two-dimensional plane. As mentioned earlier, since the three-dimensional metrics of a primary satellite and the attitude profile are typically known by the mission as part of their regular concept of operations, one can determine the nominal attitude rotation profile at TCA. We present two methods considered for the present study.

Spherical Harmonics of a 3D CAD Model using the Blender® Software

The first method of spacecraft modeling considered was the ingestion of a high-fidelity three-dimensional model from NASA's public website www.nasa3d.arc.nasa.gov/models that is

typically used to provide models for 3-D printing, and export of the vertices of each point on the spacecraft as a data file via a software tool known as Blender*. The idea behind using Blender was to ingest the spacecraft CAD model, as shown in Figure 3(a), and then export an ASCII *.obj* file that contains the coordinates in X , Y and Z . Given Blender's high fidelity three-dimensional modeling capabilities, the finite detailed information of the vertices were typically captured at a very refined level that segmented a spacecraft's plate into smaller resolutions. This approach resulted in a significantly large number of vertex coordinates that both went far beyond the resolution needed for this purpose, as well as substantially increasing computational costs.



(a) Spacecraft 3D model import to Blender

(b) Spacecraft design using Blender

Figure 3. 3D Spacecraft modeling for encounter plane projection

A second approach involved constructing a simpler generalized model that approximated the general shape of the satellite as shown in 2(b) using the Blender Software. In this approach, the vertices were extracted by approximating each plate using two-triangles, which is a reasonable approximation for an N-plate design. In order to capture the projected shape of the spacecraft in the conjunction plane, one line of attack involved investigating the use of spherical harmonics to approximate the projected cross sectional area⁴. The spherical harmonics are a combination of orthonormal functions, which means on a given unit sphere, any square integrable function $f(\theta, \lambda)$ can be expanded as a linear combination of these functions, as shown in Equation 1 and is explained in detail by Farrés⁴ and Vallado⁵.

$$f(\theta, \lambda) = \sum_{n=0}^{\infty} \sum_{m=0}^n [A_{nm} \cos m\lambda + B_{nm} \sin m\lambda] \bar{P}_{nm}(\cos \theta) \quad (1)$$

A_{nm} and B_{nm} are the Fourier coefficients and \bar{P}_{nm} are the normalized Legendre Polynomials⁵. Farrés demonstrates the innovative use of spherical harmonics to calculate the force exerted by solar radiation pressure (SRP) on a cross sectional area of a spacecraft; the sun-line for SRP could be reconsidered by analogy as the relative velocity vector for CA. In the spherical harmonics approximation, the longitude θ and latitude λ angles can be used to define the satellite's attitude with respect to the Sun-line, and α and β in Figure 4, are calculated from the attitude information of the primary spacecraft (assuming a spherical model for the secondary spacecraft).

*J.L. T. Roosendaal, "www.blender.org," Stichting Blender Foundation, 2007

An operator would then input the given attitude profile at TCA to calculate the cross-sectional area in the encounter plane. The Fourier and Legendre Polynomials would be implemented only once, after a spacecraft's bus design is finalized prior to launch.

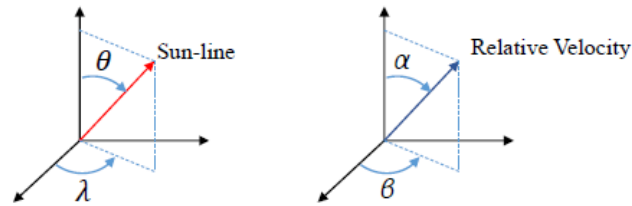
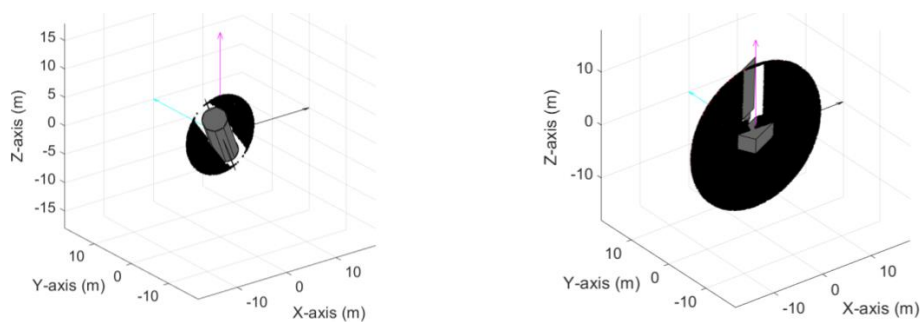


Figure 4. Primary Spacecraft in the body fixed reference frame. Left: Solar Radiation Pressure capture; Right: Cross-sectional Area capture

To use this polynomial approach, one requires the spacecraft's attitude profile in the body-fixed frame and rotated with respect to the relative velocity vector's axis. This method would provide as accurate a cross-sectional value as one could get. However, in order to employ it sensibly, it would be beneficial to incorporate the P_c calculation with the spherical harmonics set of orthonormal functions, an idea to be revisited for future work.

N-Plates polygons using MATLAB®

The second method considered is relatively simpler and straightforwardly implemented in MATLAB®. The generalized 3-D spacecraft model's dimensions are outlined as flat plates, with the origin of the coordinate frame approximately placed at the center of figure of the spacecraft bus in order to approximately coincide with the center of mass⁸. This is an important aspect when modeling un-symmetrical spacecraft, because astrodynamics models represent the position of the spacecraft at its center of mass. Therefore, when projecting the spacecraft unto the encounter plane, there could be several interpretations of the circumscribing circle depending on the spacecraft model that could affect the outcome of the HBR definition and thus the computed P_c .



(a) Hubble Space Telescope 3D Satellite Model (b) AURA 3D Satellite Model

Figure 5. Spacecraft design in MATLAB®

In Figure 5(a), a random projection of the Hubble Space Telescope (HST) on the encounter plane reveals the projected cross-sectional area intersecting the scattered black dots in the circumscribing circle. With the center of the figure at the center of the circumscribing circle, the radius of the circumscribing circle grazes the extremities of the projected shape. Figure 5(b), shows the Aura satellite's projection with the radius defined from the center of the figure to the uttermost extremity. Now given that the Aura spacecraft is not symmetric, the lower semi-circle can be considered as excess-area in the definition of the total HBR. In Table 1, the variability in projected areas and the defined circles for the primary spacecraft (that end up constructing the HBR when including the secondary object) is shown.

Table 1. Projected Cross-sectional area vs defined circumscribing circle of a Primary Spacecraft.

	Projected Cross-Sectional Area	Defined Cricumscribing Circle
HST Area (m^2)	67.1	150.7
Aura Area (m^2)	145.7	555.7

The extremely large differences between the actual spacecraft projected areas and those of the projected circumscribing circle certainly suggest notable differences expected in the calculated P_c , given that P_c scales with projected spacecraft combined area.

Let us consider a sample symmetric spacecraft that is rotated on a conjunction plane with the two angles α and β (as shown in Figure 4) varying from 0 to 2π . The span of these rotations results in a wide range of circumscribing circles that in turn vary the defined HBR. The range of HBR values will always depend on the shape of the spacecraft and its resultant projected area on the conjunction plane. From the various attitude spans about the primary spacecraft, a resulting circumscribing HBR and area values are obtained as summarized in Table 2 and shown in Figure 6. For many spacecraft, a circular projection would result in relatively less variance in the HBR values. However, for some spacecraft with non-symmetrical shapes, the HBR would vary widely with the particular projection situation.

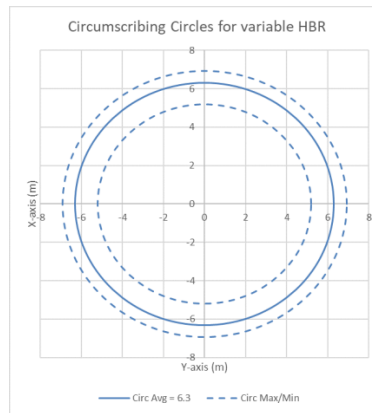


Figure 6. Hard-body Radius and Covariance schematic for Probability of Collision calculations.

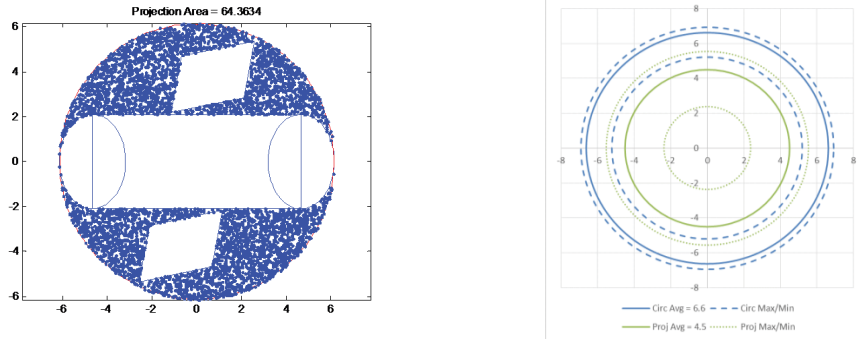
Table 2. Projected Cross-sectional area vs defined circumscribing circle of a Primary Spacecraft.

Circumscribing Circle	Minimum	Average	Maximum
Radius (<i>m</i>)	5.2	6.3	6.9
Area (<i>m</i> ²)	84.94	124.69	149.57

If one wishes to calculate the precise projected area of an irregular shape, one can proceed through a Monte Carlo tallying approach. This approach generates a number of points uniformly distributed unto a circumscribing circle, and the ratio of the number of points that hit the polygon to the ratio of total points in the circle is used to calculate the equivalent polygonal area of the projected spacecraft unto the conjunction plane. In generating a uniformly-distributed number of points in a circle or sphere, a concentrated distribution tends to occur near the poles, thus resulting in a non-uniform distribution and, in turn, inaccurate results. Using the uniform sphere distribution relationships shown in Equation (2) enables the generation of uniformly-distributed points on a sphere or a circle where *u*, *v* and *w* are the random points in the Cartesian frame.

$$\begin{aligned}\theta &= 2\pi u \\ \phi &= \sin^{-1}(2v - 1) \\ v &= 2\pi w\end{aligned}\tag{2}$$

If we evaluate the projected polygon's actual projected area and represent this as an equivalent circular area (See Figure 7(a), the projected circle's area can be plotted as shown in Figure 7b). Shown in a solid green line is the equivalent projected polygonal area realized as a circle and the dotted green lines show the maximum and minimum areas based on the varied attitudes. The solid blue line is the average area of the circumscribing circles based on the varying attitudes, and the dotted blue lines show the maximum and minimum areas based on the varied attitudes.



(a) Projected area polygon on conjunction plane (b) Circumscribed vs Projected Radius

Figure 7. Circumscribed circles vs projected-area equivalent circles.

CROSS-SECTIONAL AREA AND HARD BODY RADIUS PROFILES

In this section, we will summarize the five different cross-sectional area and HBR definitions considered and examine their implications by recalculating the Pc values for a set of historical conjunction data using the different HBR values that each approach yields. To do this, the following information needs to be assembled.

For any spacecraft 3D N-plate model, one can constrain and therefore specify the solar panel positions to be sun-ward pointing and incorporate that information in formulating the pre-projection spacecraft attitude. If the solar array pointing information for a particular spacecraft is available, then it can be ingested in the projection calculations; otherwise, SPICE kernel files[‡] may be used. The SPICE system includes geometric parameters of celestial bodies at selected times; these files are used to provide the positions and velocities of the Earth with respect to the Sun, permitting computation of the rotational angles needed to preserve a normal orientation with respect to the sun vector.

The state and covariance information of the primary spacecraft needed for the Pc calculation can be extracted from the standard Conjunction Data Message (CDM) describing a predicted close approach, along with the TCA. The TCA is then used to parse through the attitude *.FDD* ASCII text files to read-in the spacecraft attitude yaw, roll, and pitch angles. The solar panels' plate baseline profile with respect to the spacecraft's attitude is known. The rotational relationship from the spacecraft's current attitude and its projection unto the encounter plane is used to determine the maximum resulting angle of the solar panels pointing towards the sun, as illustrated in Figure 8.

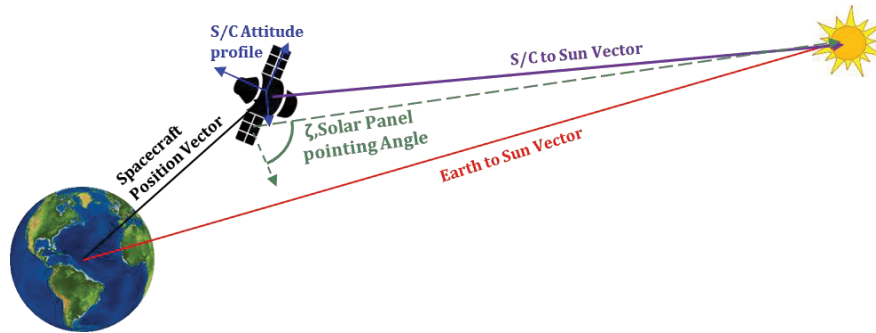


Figure 8. Illustration of SPICE kernel files used to obtain pointing vectors to orient the solar panels to maximize exposure to the Sun.

Most spacecraft maintain a given attitude based on the science goals of the mission. For the cases examined in this study, the primary spacecraft maintains a nominal Nadir pointing profile and thus should not require an operator to always calculate the primary spacecraft's orientation at TCA, thus saving the computational cost that would be needed to parse the attitude file.

[‡]The Navigation and Ancillary Information Facility, <https://naif.jpl.nasa.gov/naif/>

This proves that the varying attitudes of the spacecraft can in turn change the total projected area and, depending on how the area is defined, can widely vary the defined HBR and the resulting calculated Pc. This method also assumes that a spherical volume or circumscribing circle on the encounter plane is the best way to capture the spacecraft's area. One could also calculate the Pc using surface area or line integral methods over the projected polygon area. The Pc can be evaluated over the bounded shape evaluated at the indices of the projected shape on the conjunction plane, thus leading to the several approaches that one could use to define the HBR and assess the Pc value at TCA. Five profile methods that can be used to define the HBR and in turn calculate the Pc are presented herein.

These approaches introduce the variable ways a 2D Pc can be evaluated and indicate how much a close approach mitigation maneuver decision could vary given the wide range of Pc values obtained. With the increase of resident space objects, this analysis can provide a new way of re-defining how the probability of collision can be characterized in order to improve the decision-making strategy.

Profile 1: A Fixed Hard Body Radius (HBR)

A common approach to define a HBR, used more widely in the past but still encountered, is to choose a relatively large spherical size about the primary as a HBR. The size of this sphere is based to some degree on the size of the primary (circumscribing sphere) and augmented to account for the expected size of a large(r) secondary object, However usually the actual size selected for the secondary does not emerge from any particular size analysis. It was common previously to assign a blanket value of 20m as the combined HBR value, and that is the value that is adopted for this profile.

The 2D Pc is integrated over the HBR and is given in the Equation (3) below ^{6,7}

$$Pc = \frac{1}{2\pi\sigma_x\sigma_y} \int_{-HBR}^{HBR} \int_{-\sqrt{HBR^2-x^2}}^{\sqrt{HBR^2-x^2}} \exp\left[\left(-\frac{1}{2}\right)\left(\left(\frac{x+x_m}{\sigma_x}\right)^2 + \left(\frac{y+y_m}{\sigma_y}\right)^2\right)\right] dy dx \quad (3)$$

Profile 2: Circumscribing circle with secondary

In this profile, the maximum vertex of the primary spacecraft from the center of the spacecraft bus is used to construct the primary radius. This is added to a radius of 1.5m for the secondary object (a value identified from a CARA study to encompass an acceptably large percentage of actual secondary object sizes for space debris) to construct the HBR of the total circumscribing circle. The total HBR is the sum of R_1 and R_2 , as shown in Figure 9. The 2D Pc calculation for this profile is identical to the formula given in Equation (3) for Profile 1.

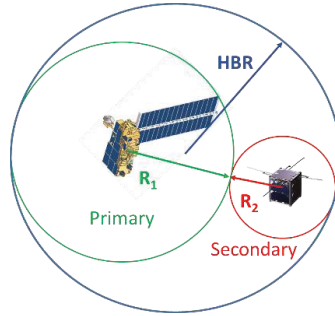


Figure 9. Circumscribing circle encompassing the maximum vertex of the primary spacecraft (R_1) and a radius of 1.5m (R_2) of the secondary object.

Profile 3: Event-specific projected area with circumscribing circle.

The event-specific projected area takes the polygon shape on the encounter plane and circumscribes a circle around that shape. In Figure 10, the primary spacecraft's blue circumscribing circle HBR is added to the red circle (secondary) to construct the total HBR (black circle). In this profile consideration, the attitude information at TCA is incorporated to ensure the accurate representation of the resulting cross-sectional area on the encounter plane and the required SPICE kernel files (as illustrated in Figure 8), are used for the correct pointing of the solar panels towards the Sun. Ultimately, the total HBR is expected to be much smaller than those computed for profiles 1 and 2, depending on the direction of the relative velocity vector that is also subject to the velocity vector of the secondary object.

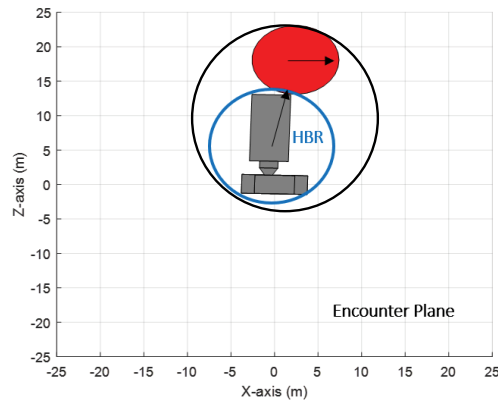


Figure 10. Event Specific (TCA) projected area with circumscribing circle (Blue Circle for Primary, and Red for Secondary)

Profile 4: Primary spacecraft projected area realized as a circle

The primary spacecraft at TCA is projected onto the conjunction plane as an equivalent circle with the same area as the primary spacecraft. The equivalent circular area is computed by using the rotation matrices below to map the plates that make up the spacecraft into the encounter plane. Let r_1 and r_2 be the position vectors and v_1 and v_2 be the velocity vectors for the primary and secondary spacecraft respectively. Using a position covariance in the radial, in-track, and cross-track (RIC) frame, Cov_{RIC_i} and Cov_{RIC_s} , we derive the rotation matrix M_{xyz} that can be decomposed to the matrix that will project the uncertainty and relative distance on the encounter plane XZ as follows:

Construct relative vectors:

$$\begin{aligned} r &= r_1 - r_2 \\ v &= v_1 - v_2 \\ h &= r \times v \end{aligned} \quad (4)$$

Construct the relative encounter frames:

$$\begin{aligned} y &= v / \text{norm}(v) \\ z &= h / \text{norm}(h) \\ x &= y \times z \end{aligned} \quad (5)$$

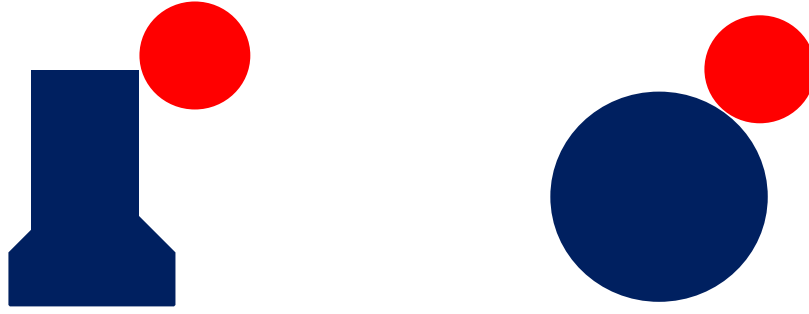
Transform attitude from ECI into the XYZ encounter frame for primary and secondary objects, where $i = \{1,2\}$:

$$\begin{aligned} M_{XYZ} &= [x \ y \ z]^T \\ Cov_{XYZ_i} &= M_{XYZ} * Cov_{RIC_i} * M_{XYZ} \end{aligned} \quad (6)$$

The covariance is then projected unto the XZ -encounter plane:

$$Cov_{XZ_i} = \begin{bmatrix} 1 & 0 & 0 \\ 0 & 0 & 1 \end{bmatrix} * Cov_{XYZ_i} * \begin{bmatrix} 1 & 0 & 0 \\ 0 & 0 & 1 \end{bmatrix}^T \quad (7)$$

The areas projected from the plates onto the plane result into a polygon shape on the encounter plane, as shown in the blue polygon in Figure 11(a). The radius of a circle of equivalent area is determined from the simple circular area equation πr^2 (made to have an equivalent area as the projected polygon, as shown in Figure 11(b)). The total HBR used for this profile then includes both the radius of the blue circle in Figure 11(b) and the secondary object (red circle) with a radius set at 1.5m.



(a) Primary spacecraft maximized projected area (Blue Polygon)

(b) Equivalent area maximized as a circle (Blue Circle)

Figure 11. Primary spacecraft maximized projected area realized as a circle (Blue) and the secondary object with a 1.5m radius

Profile 5: Event projected polygon area.

Here we evaluate the P_c by integrating over the polygon area using the limits of integration based on the edges of the polygon on the encounter plane as shown in Figure 12. The secondary object is considered by incorporating the bias-offset from the center of the secondary's circle. Using numerical integration methods, Equation (8) is evaluated over both the polygon shape and the circle on the encounter plane to obtain the final P_c value at TCA.

Using a polygon contour integral over the area, the 2D- P_c can be evaluated as shown in Equation (4) and illustrated in Figure 12:

$$P_c = \frac{1}{2\pi\sigma_x\sigma_z} \int_{X_1}^{X_N} \int_{Z_1}^{Z_N} \exp \left[\left(-\frac{1}{2} \right) \left(\left(\frac{X-X_m}{\sigma_x} \right)^2 + \left(\frac{Z-Z_m}{\sigma_z} \right)^2 \right) \right] dZdX \quad (8)$$

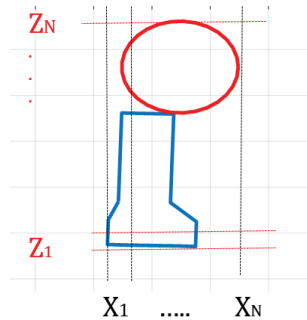


Figure 12. The projected spacecraft (Blue Polygon) and the secondary object (Red Circle) are computed separately and added together to produce the final P_c over both objects' areas in the conjunction plane.

The double integral integrates the 2D P_c function over the polygon. The vertices $(X_1, Z_1), (X_2, Z_2), \dots, (X_N, Z_N)$ are applied as limits of integration in Equation (8) in a clockwise or counter-clockwise order to close the polygon.

PROBABILITY OF COLLISION RANGE VALUES FROM HARD BODY RADIUS PROFILE ANALYSES

In this section, a six months' history of conjunction information is examined for three NASA payloads in near-circular, 700km orbits: Spacecraft A, Spacecraft B, and Spacecraft C, extracting conjunctions from which the P_c , calculated using a 20 m HBR, exceeds $1E-05$. Each conjunction was then processed using all five of the HBR profiles described above. Profile 1's calculated P_c was then compared with the rest of the HBR profiles to assess the degree of departure, profile by profile, from the baseline P_c produced using Profile 1. The results are shown as quad charts of scatter plots in Figure 13, in which Profiles 2-5 are compared to the Profile 1 results. The P_c values for the profiles being compared are shown on the two axes, and two "color" boundaries are also shown as dotted lines on the plots. A red line at profile 2= $4.4E-04$ maps to the current CARA "red" threshold at which a mitigation action will typically be considered. The green dotted line at profile 2= $1E-05$ defines a "yellow" threshold at which mitigation action planning should be pursued in anticipation of the possibility of the P_c values' increasing to the red threshold as new tracking data is received as time approaches the TCA. The color of each data point reflects the P_c produced by the profile being compared to the baseline (profile 2-5, as appropriate).

The magenta dots represent the "Red Category" values of $P_c > 4.4e-4$ and above the dotted red line in Figures 13 and 14, as calculated by the profiles defined in the y-axis. The blue dots represent the "Yellow Category" of P_c values between $4.4e-4 < P_c < 1e-5$, and illustrated in Figures 13 and 14, between the dotted red and green lines. The cyan dots, represent values of $P_c < 1e-5$ (also known as the "Green Category") as calculated by the profiles defined on the y-axis, under the dotted-green line.

In the quadcharts in Figure 13, one can easily see the depression of the P_c value as more sophisticated HBR determination methods are applied advancing from Profile 2 through Profile 5 as compared to the P_c results from Profile 1. What is taking place is the subsequent decrease of the projected cross-sectional area that also decreases the defined HBR (where applicable) and the resulting

Pc. As the profiles advance from 2 to 5, fewer and fewer magenta dots occur above the red-dotted line and to the right of the solid-vertical line representing Profile 1's calculated and categorized CDMs in the red category.

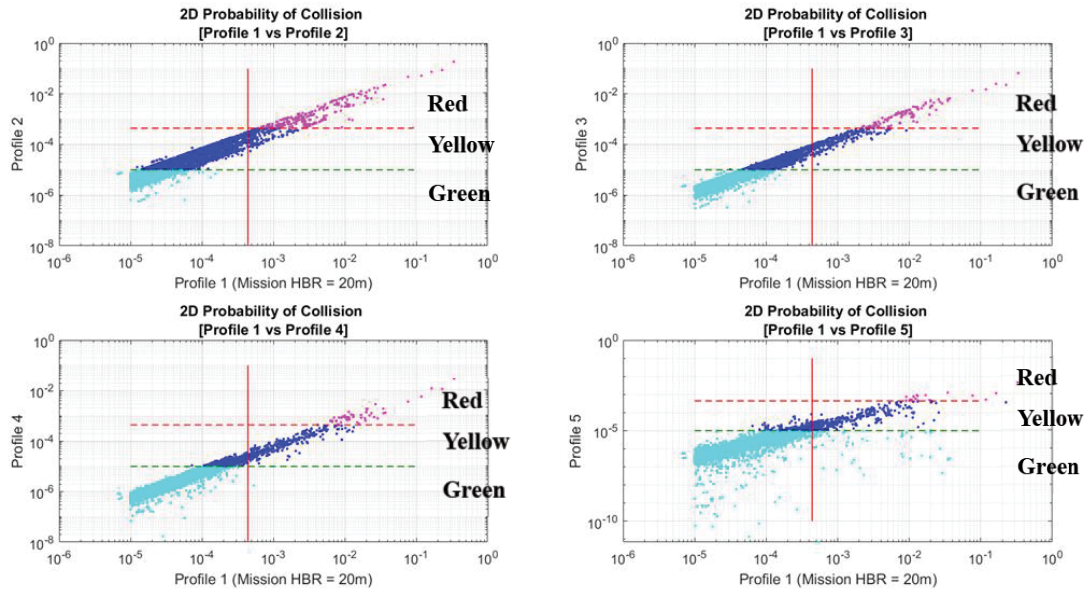


Figure 13. Calculated Pc from various HBR profiles in the conjunction plane compared to Profile 1.

Table 3 summarizes the percentage of cases in which the Pc is decremented compared to a Profile 1 red category to a yellow (or green) category by applying the other profiles.

Table 3. Percentages of Profile 1 that decrement from a Red Category ($P_c > 4.4e-4$) to a Yellow Category ($4.4e-4 < P_c < 1e-5$) in the HBR Profiles.

% of Red Category Decrement	Profile 2	Profile 3	Profile 4	Profile 5
Profile 1	43.97%	73.05%	87.49%	95.98%

In Figure 14, a similar comparison is considered using the reference Profile 2 as the baseline to which the other profiles are compared. Profile 2 is the current most common approach used in operations when considering a HBR to use for conjunction analysis. Since Profile 2 considers a tighter circumscribing circle, fewer decremented Pc values occur, as expected. The corresponding percentage values in Table 4 show a lesser degree of Pc decrementation compared to the results in Table 3. This result highlights the importance of using an accurate HBR definition for mission specific operations versus using an arbitrary fixed HBR value to reduce inherent uncertainty in the calculation and obtain a realistic Pc value for decision-making.

As one would expect, when known and accurate attitude information can be incorporated during operations, the final Pc can be anticipated to be significantly lower than using an arbitrary fixed HBR value.

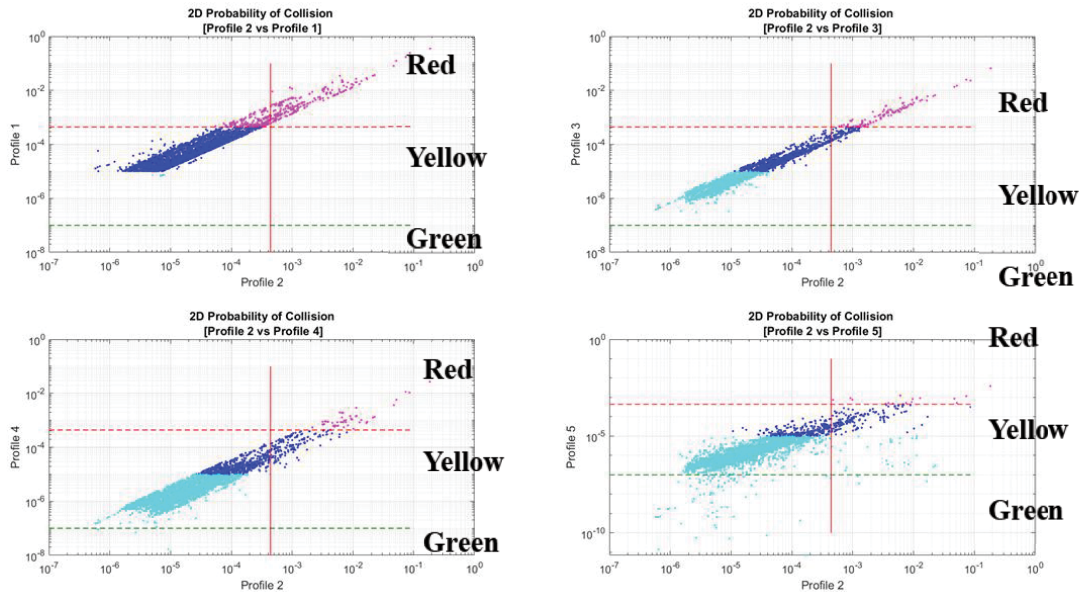


Figure 14. Calculated Pc from various HBR profiles in the conjunction plane compared to Profile 2.

Table 4. Percentages of Profile 2 that decremented from a Red Category ($P_c > 4.4e-4$) to a Yellow Category ($4.4e-4 < P_c < 1e-5$) in the HBR Profiles.

% of Red Category Decrement	Profile 1	Profile 3	Profile 4	Profile 5
Profile 2	0%	51.90%	78.48%	92.83%

CONCLUSION

This analysis has shown the advantages and disadvantages of employing any one of many different HBR definitions/constructions in calculating the Pc. In the event that a mission's attitude information is readily available with reasonable accuracy levels, incorporating a variable HBR based on the actual projected satellite size is shown to be extremely beneficial in collision avoidance decision making by minimizing the calculated severity of conjunction events by minimizing the uncertainty inherent in the Pc computation.

Additionally, the profiles presented herein are generalized HBR representations. It is obvious that the attitude profile for a spacecraft is not deterministic and undergoes various non-conservative perturbations that affect the accuracies of the attitude information. However, the objective of this work was to demonstrate the benefits of using the best representative HBR value possible in order to avoid unnecessary risk mitigation maneuvers and overhead costs for risk mitigation planning.

ACKNOWLEDGMENTS

The authors acknowledge with gratitude the contributions of former Omitron employee Lauren Johnson on an earlier version of this study.

REFERENCES

- ¹ K. Chan, *Spacecraft Collision Probability*. El Segundo, California: The Aerospace Press, El segundo, California and American Insititute of Aeronautics and Astronautics, Inc, Reston, Virginia, March 2008.
- ² K. Chan, "International Space Station Collision Probability," *The Aerospace Corporation, Chantilly, VA, USA*, 2009
- ³ M. Matney, "How to calculate the average cross-sectional area." *The Orbital Debris Quarterly News*. Vol. 8, No. 2, 2004, pp. 7.
- ⁴ A. Farrés, D. Folta and C. Webster, "Using spherical harmonics to model solar radiation pressure accelerations." *2017 AAS/AIAA Astrodynamics Specialist Conference*, (Preprint) AAS 17-780
- ⁵ D.A. Vallado, *Fundamentals of Astrodynamics and Applications*. El Segundo, California: Microcosm Press, 2nd ed., 2004
- ⁶ M. Akella and K. Alfriend, "The Probability of Collision Between Space Objects," *Journal of Guidance, Control and Dynamics*, Vol. 23, No. 5, 2000, pp. 769–772.
- ⁷ J. Foster and H. Estes, "A Parametric Analysis of Orbital Debris Collision Probability and Maneuver Rate for Space Vehicles," NASA/JSC-25898, 1992.
- ⁸ M.D. Hejduk and L. Johnson, "Approaches to evaluating probability of collision uncertainty," Preprint AAS 16-241, 2016.